

Dietary coconut oil lowered circulating fetuin-A levels and hepatic expression of fetuin-A in KK/TaJcl mice

Yuzuru Iizuka,^{1,*} Chikako Kitagawa,² Towa Tamura,² Hidehiro Ueshiba,¹ Satoshi Hirako,³ Toshifumi Osaka,¹ Hyounju Kim,⁴ and Naoko Yanagisawa¹

¹Department of Microbiology and Immunology, Tokyo Women's Medical University School of Medicine, 8-1 Kawada-cho, Shinjuku-ku, Tokyo 162-8666, Japan

²School of Medicine, Tokyo Women's Medical University, 8-1 Kawada-cho, Shinjuku-ku, Tokyo 162-8666, Japan

³Department of Health and Nutrition, University of Human Arts and Sciences, 1288 Magome, Iwatsuki-ku, Saitama 339-8539, Japan

⁴Department of Nutrition and Health Sciences, Faculty of Food and Nutritional Sciences, Toyo University, 48-1 Oka, Asaka-shi, Saitama 351-8510, Japan

(Received 12 September, 2024; Accepted 27 September, 2024; Released online in J-STAGE as advance publication 11 October, 2024)

Although coconut oil has attracted great attention as a functional food, enough supportive scientific evidence is lacking. In addition, the beneficial effects of coconut oil consumption on the prevention of metabolic disorders are controversial. Fetuin-A is a plasma glycoprotein secreted by hepatocytes and adipocytes. Circulating fetuin-A levels relate to insulin resistance due to macrophage-mediated adipose tissue inflammation. This study demonstrated that coconut oil feeding significantly down-regulated the hepatic expression of fetuin-A and reduced its plasma level in KK mice—an obese diabetic model animal. The expression of monocyte chemoattractant protein-1, a potent inducer for macrophage infiltration, decreased in epididymal white adipose tissue in coconut oil-fed KK mice. The expression of CD68 and CD11c, markers of proinflammatory M1 macrophages, was significantly reduced by coconut oil feeding in epididymal white adipose tissue of KK mice. However, the mice did not exhibit improved insulin resistance. Our results may further support the potential of coconut oil as a dietary trigger that can reduce both circulating fetuin-A levels and infiltration of proinflammatory macrophages in visceral adipose tissue.

Key Words: coconut oil, type 2 diabetes, fetuin-A, adipose tissue inflammation, M1 macrophage

Coconut oil (CO) is one of the edible oils extracted from the kernel of *Cocos nucifera* L. CO is rich in medium-chain fatty acids (MCFAs), such as lauric acid (C12:0), caprylic acid (C8:0), and capric acid (C10:0).⁽¹⁾ These fatty acids are classified as saturated fatty acids and are characterized by preferential absorption directly into the portal vein and transport to the liver for rapid oxidation without storage in adipose tissue.⁽²⁾ CO has attracted attention as a functional food with anti-obesity, anti-hyperlipidemic, and other health effects in the wellness market. However, Deen *et al.*⁽³⁾ reviewed several human studies and concluded that enough evidence for weight control through CO consumption is lacking.

CO-associated antidiabetic effect is a target for health benefits. *In vivo*, CO feeding improved hyperglycemia and insulin resistance in obese or diabetic rodents.^(4–6) Insulin resistance is caused by obesity-induced chronic low-grade inflammation in adipose tissue. The expansion of white adipose tissue (WAT) associated with obesity induces secretion of proinflammatory cytokines and chemokines, such as tumor-necrosis factor- α (TNF- α), interleukin-6 (IL-6), and monocyte chemoattractant protein-1 (MCP-1).⁽⁷⁾ In high-fat diet-fed rodents, CO supplementation lowered circulating proinflammatory cytokine levels and adipose

tissue inflammation.^(8,9) Systematic review and meta-analysis have indicated that CO-derived fat had no beneficial effects on acute or long-term glycemic control.⁽¹⁰⁾ Therefore, the efficacy of CO consumption in preventing diabetes is controversial.

Glucose and lipid metabolism are partially regulated by the hepatokine fetuin-A, which is a plasma glycoprotein secreted from both hepatocytes and adipocytes, triggering adipose tissue inflammation and insulin resistance.⁽¹¹⁾ Hyperglycemia and hyperlipidemia are associated with the upregulation of fetuin-A expression in the liver, and the complex of fetuin-A with free fatty acid (FFA) activates inflammatory signaling and insulin resistance in adipocytes through toll-like receptor 4 (TLR4).^(12–14) In addition, a high level of circulating fetuin-A is related to nonalcoholic fatty liver disease through the induction of insulin resistance in skeletal muscles and hepatocytes.⁽¹⁵⁾ Therefore, fetuin-A is a potential biomarker and therapeutic target for type 2 diabetes, dyslipidemia, fatty liver, and other related metabolic disorders. Several studies have demonstrated that functional food ingredients, such as curcumin and resveratrol, could regulate the production and circulating levels of fetuin-A.^(16,17) The synthesis of fetuin-A is mediated by signal transduction through nuclear factor-kappa B (NF- κ B), a key transcription factor for the inflammatory response.⁽¹²⁾ However, the effects of CO consumption on NF- κ B and fetuin-A associated with glucose and lipid metabolism are unclear.

Therefore, we focused on the effects of CO on circulating fetuin-A and its production in the liver and adipose tissue pertaining to metabolic disorders associated with obesity, such as type 2 diabetes, hyperlipidemia, and fatty liver. To evaluate if CO is a healthy edible oil, this study examined the effects of CO consumption on the relationship between fetuin-A production and obesity-related metabolic disorders using KK/TaJcl (KK) mice as obese diabetic model animals and C57BL/6Jcl (BL6) mice as normal controls.

Material and Methods

Animals and diets. BL6 and KK male mice (aged 6 weeks) were purchased from CLEA Japan (Tokyo, Japan) and housed individually in a controlled environment at a temperature of $23 \pm 1^\circ\text{C}$, humidity of $50 \pm 10\%$, and a 12-h light-dark cycle. The mice were allowed free access to water and a commercial chow diet (MF; Oriental Yeast, Tokyo, Japan) and were acclimated

*To whom correspondence should be addressed.
E-mail: iizuka.yuzuru@twmu.ac.jp

for 1 week to stabilize metabolic conditions. At 7 weeks of age, BL6 and KK mice were divided into two groups ($n = 5$) based on body weight and administered the following experimental diets: lard/safflower oil (LSO) and CO, for 8 weeks. The LSO diet contained 25 energy% (en%) from lard (Oriental Yeast) and safflower oil (Benibana Foods, Tokyo, Japan) in a mixture (4:6), as described.⁽¹⁸⁾ The CO diet was prepared by mixing 20 en% CO (Fujifilm Wako Pure Chemical, Osaka, Japan) with 5 en% LSO. The experimental diets contained 10.5% (wt:wt) of dietary fats. The diet composition and fatty acid composition of the experimental diet are listed in Supplemental Table 1 and 2*, respectively. CO contains 60.2% MCFAs, such as C8:0, C10:0, and C12:0, based on total fatty acid content. The analysis of fatty acids in the experimental diet was conducted by Japan Food Research Laboratories (Tokyo, Japan). During the experimental period, we administered these diets to each mouse every other day and monitored food intake. At the start of the experiments and at 4, 6, and 8 weeks, blood glucose levels were measured from the tail vein of mice fasted overnight for 12 h using a blood glucose monitoring system (One Touch Ultra Vue; Life scan IP Holdings, Malvern, PA). Then, the mice were euthanized by isoflurane. Blood samples were collected from the heart with heparin under anesthesia and centrifuged ($700 \times g$, 4°C, 15 min) to separate plasma. Samples of tissues, including the liver, epididymal WAT (eWAT), inguinal WAT (iWAT), and interscapular brown adipose tissue (BAT), were weighed and frozen in liquid nitrogen. All samples were stored at -80°C until analysis. All animal experiments were performed in accordance with “the recommendations in the Guide for the Care and Use of Laboratory Animals of Tokyo Women’s Medical University (permission No. AE22-066-C)”.

Biochemical analyses. Plasma triglyceride (TG) and FFA levels were determined using Triglyceride E-Test kit and NEFA C-test kit (Fujifilm Wako Pure Chemical) by spectrophotometric methods, respectively. Plasma insulin levels were measured using an enzyme-linked immunosorbent assay (ELISA) kit (Ultra-sensitive mouse insulin ELISA kit; Morinaga Institute of Biological Science, Tokyo, Japan). The homeostasis model assessment of insulin resistance (HOMA-IR) index was calculated as described.⁽¹⁸⁾ Plasma fetuin-A and leptin were measured using mouse Fetuin-A/AHSG Quantikine ELISA Kit (R&D Systems, Minneapolis, MN) and Mouse/Rat Leptin Quantikine ELISA Kit (R&D Systems), respectively. Total lipids from the liver were extracted according to the method of Folch *et al.*⁽¹⁹⁾ Hepatic TG content was measured using Triglyceride E-Test kit (Fujifilm Wako Pure Chemical).

Quantitative determination of proinflammatory cytokines. To estimate proinflammatory cytokines in eWAT, tissues were homogenized with RIPA buffer containing a protease inhibitor cocktail (Roche, Mannheim, Germany) without sodium dodecyl sulfate. The tissue homogenates were centrifuged at $15,000 \times g$ at 4°C for 10 min. The supernatants were collected, and protein concentrations in the supernatants were measured using the Bradford assay. The quantitative determination of TNF- α and IL-6 in eWAT was performed using LEGENDplex (BioLegend, San Diego, CA) and CytoFLEX Flow Cytometer (Beckman Coulter Life Sciences, Indianapolis, IN), according to the manufacturer’s instructions. Data were analyzed using the online QOGNIT LEGENDplex program. MCP-1 level was determined using Mouse CCL2/JE/MCP-1 Quantikine ELISA Kit (R&D Systems).

Western blotting. Total protein was extracted from the liver and eWAT using lysis buffer containing a protease inhibitor cocktail (Roche). The homogenates were centrifuged at $18,000 \times g$ at 4°C for 30 min. Nuclear proteins were isolated using a nuclear extraction kit, according to the manufacturer’s instructions (Active Motif, Carlsbad, CA). The concentration of protein in the supernatant was measured by the Bradford assay. The protein samples were mixed with a sample loading buffer and

separated using 10% sodium dodecyl sulfate polyacrylamide gel electrophoresis. The membranes were blocked with 5% BSA or nonfat dry milk for 1 h at room temperature and incubated overnight at 4°C with the primary antibodies (described in Supplemental Table 3*). Then, the membranes were incubated with horseradish peroxidase-conjugated anti-rabbit (#7074, 1:2,000; Cell Signaling Technology, Danvers, MA), anti-goat (sc-2768; Santa Cruz Biotechnology, Dallas, TX), and anti-mouse immunoglobulin G (ab131368, 1:4,000; Abcam, Cambridge, UK) antibodies for 1 h at room temperature. Protein bands were detected using a chemiluminescence reagent (Clarity Western ECL Substrate; Bio-Rad, Hercules, CA) and AE-9300H Ez-capture MG System (ATTO, Tokyo, Japan). The chemiluminescence intensity of bands was quantified using ImageJ software, ver. 1.52a (Wayne Rasband, NIH).

Morphological analysis. eWAT samples were fixed with 10% neutral buffered formalin (Muto Pure Chemicals, Tokyo, Japan) and embedded in paraffin. The paraffin blocks were cut into 5- μ m sections for immunohistochemical analysis. The sections were deparaffinized, rehydrated, and heated in Tris-EDTA buffer (pH 9.0) for 20 min at 121°C for antigen retrieval. Endogenous peroxidase activity was blocked using BLOXALL Endogenous Blocking Solution (Vector Laboratories, Newark, CA), according to the manufacturer’s instructions. Nonspecific antibody binding was blocked using 2.5% normal horse serum for 20 min at room temperature. The sections were stained at 4°C overnight with primary antibodies against CD68 (28058-1-AP, 1:1,000; Proteintech Group, Rosemont, IL) or CD11c (#97585, 1:200; Cell Signaling Technology) diluted with normal blocking serum. ImmPRESS HRP Horse Anti-Rabbit IgG Polymer Detection Kit (Vector Laboratories) was used as the secondary antibody, according to the manufacturer’s instructions. Immunoreactivity was visualized using 3,3'-diaminobenzidine substrate chromogen (Dako, Glostrup, Denmark). Finally, the sections were counterstained with hematoxylin and scanned with a Biorevo BZ9000 microscopy (Keyence, Osaka, Japan).

Statistical analysis. Data are presented as mean \pm SD. Comparisons between the LSO and CO groups of the same strain were carried out using the unpaired Student’s *t* test. We defined *p* values of <0.05 as statistically significant. All statistical analyses were performed using Microsoft Excel.

Results

CO feeding had no effect on obesity and fatty liver in BL6 and KK mice. Final body weight was not different between LSO and CO groups in BL6 and KK mice. The weights of eWAT and BAT significantly increased in the CO group compared with the LSO group in KK mice; however, no significant differences were observed between groups in BL6 mice. iWAT weight was not affected by CO in both BL6 and KK mice. Although liver weight was significantly higher in the CO group than the LSO group in BL6 mice, there was no difference between groups in KK mice (Table 1). The content of hepatic TG and FFA did not significantly change between LSO and CO groups in BL6 and KK mice. However, the CO diet tended to increase ($p = 0.0611$) hepatic TG compared with the LSO diet in KK mice (Table 2).

In this study, CO feeding did not affect energy intake in BL6 mice. By contrast, energy intake significantly decreased by ~8% in the CO group compared with the LSO group in KK mice (Table 1). The difference in the level of plasma leptin, a peptide hormone positively associated with body fat mass,⁽²⁰⁾ was not significant between LSO and CO groups in each strain (Table 2). Body weight, WAT weight, hepatic lipid content, and plasma leptin level were not lower in CO-fed KK mice than in LSO-fed KK mice, suggesting that the difference in energy intake between LSO and CO groups did not markedly obscure the effect of CO feeding on at least obesity and fatty liver.

*See online. <https://doi.org/10.3164/jcbs.24-160>

Table 1. Energy intake, body weight, and tissue weights

Group	C57BL/6		KK	
	LSO	CO	LSO	CO
Energy intake (kcal/day/mouse)	13.7 ± 0.4	13.9 ± 0.1	21.8 ± 1.0	20.0 ± 0.7*
Initial body weight (g)	19.3 ± 0.5	19.3 ± 0.5	24.9 ± 0.7	24.9 ± 0.6
Final body weight (g)	27.6 ± 1.1	28.8 ± 1.0	39.6 ± 1.5	39.7 ± 0.6
Liver weight (g)	0.99 ± 0.06	1.09 ± 0.06*	1.60 ± 0.18	1.77 ± 0.16
Epididymal WAT weight (g)	0.70 ± 0.12	0.78 ± 0.07	1.62 ± 0.06	1.77 ± 0.07*
Inguinal WAT weight (g)	0.45 ± 0.07	0.49 ± 0.03	1.00 ± 0.09	1.01 ± 0.08
BAT weight (g)	0.08 ± 0.01	0.07 ± 0.01	0.20 ± 0.01	0.23 ± 0.01*

Data are presented as mean ± SD (*n* = 5). *Significantly different (*p* < 0.05) between LSO and CO group in each mouse using the unpaired Student's *t* test.

Table 2. Blood glucose and biochemical parameters in the plasma and liver

Group	C57BL/6		KK	
	LSO	CO	LSO	CO
Blood glucose level (mg/dl)	160 ± 26	161 ± 11	138 ± 18	110 ± 10*
Plasma insulin level (ng/ml)	0.14 ± 0.05	0.23 ± 0.08	0.81 ± 0.22	1.11 ± 0.42
HOMA-IR	1.5 ± 0.5	2.4 ± 0.9	7.2 ± 2.5	7.7 ± 2.7
Plasma TG level (mg/dl)	64 ± 7	68 ± 9	196 ± 23	231 ± 46
Plasma FFA level (mEq/L)	1.18 ± 0.49	0.93 ± 0.34	0.74 ± 0.06	0.72 ± 0.12
Plasma fetuin-A level (μg/ml)	79.3 ± 6.1	76.3 ± 1.5	96.2 ± 4.4	84.2 ± 3.1*
Plasma leptin level (ng/ml)	5.4 ± 1.0	5.4 ± 1.2	65.3 ± 4.3	51.7 ± 15.6
Liver TG level (mg/g liver)	38.8 ± 5.6	45.7 ± 7.1	66.1 ± 9.1	85.9 ± 18.1
Liver FFA level (mEq/g liver)	0.004 ± 0.001	0.006 ± 0.002	0.010 ± 0.005	0.020 ± 0.007*

Data are presented as mean ± SD (*n* = 4–5). *Significant difference (*p* < 0.05) between LSO and CO groups in each mouse was evaluated using the unpaired Student's *t* test.

Duration of antihyperglycemic effect due to CO feeding varied with the health of mice.

We evaluated the effects of CO feeding on glucose metabolism in BL6 and KK mice. In KK mice, blood glucose was significantly lower in the CO group than in the LSO group from 4 to 8 weeks. In BL6 mice, blood glucose significantly decreased in the CO group compared with the LSO group at 4 and 6 weeks; however, there were no difference between the groups at 8 weeks (Fig. 1). At the end of the experiment, the hepatic expression of glucose-6-phosphatase (G6Pase) and phosphoenolpyruvate carboxykinase (PEPCK)—rate-limiting enzymes of gluconeogenesis—was significantly downregulated in the CO group compared with the LSO group in KK mice. In BL6 mice, no significant differences were observed in the hepatic expression of G6Pase and PEPCK (Fig. 2C and D). Although the antihyperglycemic effect of CO feeding was seen in obese KK mice, the plasma insulin levels and HOMA-IR indices were unaffected by dietary fat in each strain (Table 2).

CO feeding decreased plasma fetuin-A level and fetuin-A production in the liver associated with suppressing the nuclear translocation of NF-κB in KK mice. Plasma fetuin-A level was significantly lower in the CO group than the LSO group in KK mice; however, there was no difference between the groups in BL6 mice (Table 2). Consistently, the expression of fetuin-A and the nuclear abundance of NF-κB in the liver were significantly decreased in the CO group compared with the LSO group in KK mice (Fig. 2J and K). In the CO group of KK mice, NF-κB was predominately localized to the cytosol in liver cells (Fig. 2L). By contrast, no significant changes were observed in the expression of fetuin-A and the cellular localization of NF-κB in the nucleus and cytosol between groups in the eWAT of KK mice (Fig. 3C, G, and H). In BL6 mice, fetuin-A expression as

well as nuclear translocation of NF-κB were unaffected by CO feeding in the liver (Fig. 2J and K) and eWAT (Fig. 3C and G). As a factor regulating the translocation of NF-κB to the nucleus in eWAT, the phosphorylation of extracellular signal-regulated kinases 1 and 2 (ERK1/2) was not affected by CO feeding in both KK and BL6 mice (Fig. 2I). The expression of TLR4, a critical receptor for NF-κB signaling, was unchanged by CO feeding in each strain (Fig. 3D).

CO feeding induced lipogenesis-related hepatic expression of proteins in KK mice. We examined whether CO had an impact on lipid metabolism in BL6 and KK mice. There was no significant difference in plasma TG and FFA levels between groups in each strain (Table 2). The hepatic expression of fatty acid synthase and stearoyl-CoA desaturase 1—central enzymes in the *de novo* lipogenesis pathway—was significantly upregulated in the CO group compared with the LSO group in KK mice (Fig. 2E and F). Regarding fatty acid β-oxidation-related enzymes, the expression of carnitine palmitoyl transferase 1 and medium-chain acyl-CoA dehydrogenase was unaffected by CO feeding in KK mice (Fig. 2G and H). There were no significant differences in the hepatic expression of fatty acid synthase, stearoyl-CoA desaturase 1, carnitine palmitoyl transferase 1, and medium-chain acyl-CoA dehydrogenase between groups in BL6 mice (Fig. 2 E–H).

CO feeding reduced MCP-1 protein level and macrophage migration in the eWAT of KK mice. To investigate the effect of lowering circulating fetuin-A by CO feeding on obesity-induced chronic low-grade inflammation in eWAT, we evaluated infiltrating macrophages and expression of proinflammatory cytokines and chemokines. Immunostaining of the eWAT revealed the formation of a crown-like structure by infiltrating

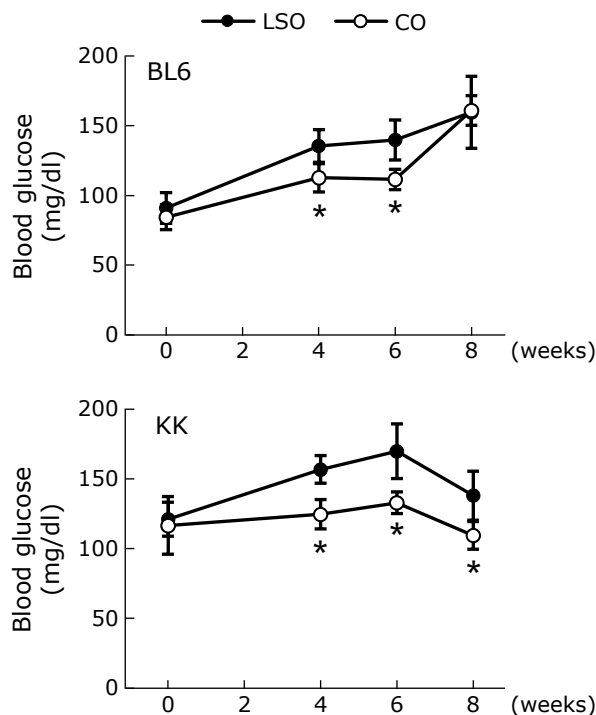


Fig. 1. Fasting blood glucose levels in 12 h-fasting C57BL/6J and KK mice during the experimental period. Data are presented as the mean \pm SD ($n = 5$). * $p < 0.05$ vs LSO group. Comparisons of two sets of data at the week of measurement in each strain were performed using the unpaired Student's *t* test. BL6, C57BL/6J mouse; CO, coconut oil; LSO, lard/safflower oil.

macrophages in the LSO group compared with the CO group in KK mice (Fig. 4A). In the immunostaining of macrophage marker and the Western blot data in eWAT of KK mice, CD68 and CD11c positive cell around the adipocyte (Fig. 4A and B) and these protein expression in tissue lysate (Fig. 3E and F) were also lower in the CO group than the LSO group, respectively. CO-fed KK mice showed a significant reduction in the expression of MCP-1 in eWAT (Fig. 3K). However, these findings were rarely observed in BL6 mice. CO feeding failed to affect eWAT expression of TNF- α and IL-6 in each strain (Fig. 3I and J).

Discussion

The effect of dietary lipids on circulating fetuin-A levels and the expression of fetuin-A in the liver have been evaluated in rodents and human,^(21–23) however, the beneficial effect of CO intake on fetuin-A abundance and obesity-related metabolic disorders is unclear. In this study, we found that CO intake decreased plasma fetuin-A levels associated with the downregulation of fetuin-A expression in the liver of KK mice with type 2 diabetes. Additionally, CO-fed KK mice showed a decrease in blood glucose after CO feeding for 4, 6, and 8 weeks. Several studies have reported that CO has a hypoglycemic effect in rodent, improving insulin resistance due to the high content of MCFAs.^(4,5,8) By contrast, we did not observe changes in plasma insulin levels and the HOMA-IR index in CO-fed KK mice, suggesting that CO intake lowered blood glucose level independent of insulin sensitivity. Gluconeogenesis is the main pathway for endogenous glucose production in the liver to maintain blood glucose during long-term fasting. However, hyperglycemia is induced by the abnormal activation of hepatic gluconeogenesis in type 2 diabetes.⁽²⁴⁾ The expression of the rate-limiting enzymes for gluconeogenesis, G6Pase and PEPCK, at the mRNA and pro-

tein level was upregulated in the liver associated with hyperglycemia in obese and diabetic mice.⁽²⁵⁾ Our findings suggest that CO intake decreased blood glucose level by downregulating the hepatic expression of G6Pase and PEPCK in KK mice. By contrast, BL6 mice did not exhibit any difference between the LSO and CO groups in blood glucose levels and the hepatic expression of gluconeogenesis-related enzymes at 8 weeks; however, blood glucose levels decreased at 4 and 6 weeks after the start of the experiment. In BL6 mice, the low levels of G6Pase and PEPCK expression may be associated with a decrease in blood glucose level. It remains unclear why the hypoglycemic effect of CO is not maintained until 8 weeks of treatment in BL6 mice. The abundance of G6Pase and PEPCK in the liver might contribute, in part, to the change in blood glucose level in CO-fed mice.

During the development of obesity, adipose tissue dynamically expands by TG accumulation into the adipocyte. This hypertrophic adipocyte secretes MCP-1 that promotes monocyte infiltration into the WAT; the monocytes differentiate into adipose tissue macrophages (ATMs).⁽²⁶⁾ ATMs are classified into the proinflammatory M1 phenotype and the anti-inflammatory M2 phenotype. Notably, M1 ATMs induce low-grade, chronic inflammation by producing several chemokines and proinflammatory cytokines that promote infiltration of other immune cells into the WAT and insulin resistance.⁽⁷⁾ Fetuin-A also acts as a chemoattractant similar to MCP-1 and polarizes ATMs from M2 to M1 in the WAT.⁽²⁷⁾ In this study, CO feeding reduced plasma fetuin-A and the expression of MCP-1 in the eWAT of KK mice. Consistently, CO-fed KK mice exhibited a decrease in CD68 expression, indicating the presence of ATMs, and CD11c as markers for M1 macrophages in the eWAT. Thus, our data indicate that CO consumption may inhibit M1 macrophage infiltration into adipose tissue, accompanied with a decrease in, at least partially, production of MCP-1 and fetuin-A. However, the level of proinflammatory cytokines, such as TNF- α and IL-6, did not change according to the fat source of diets and strains despite the scarcity of ATMs, especially in BL6 mice. The limitation of cytokine analysis is that the measurement was carried out without isolation of immune cells and adipose tissue in our study. Several cytokines are produced by both immune cells, including macrophages, and adipocytes, so that a CO diet does not change the production of proinflammatory cytokines in the entire eWAT. Additionally, it remains unclear whether the development of diet-induced inflammation in adipose tissue is different between BL6 and KK mice. However, it is difficult to explain why the levels of proinflammatory cytokine did not improve in spite of lower CD68 and CD11c expression in the eWAT of CO-fed KK mice in both cases. One possibility is that a larger decrease in M1 macrophage infiltration may be needed for the variation in the amount of proinflammatory cytokines.

Circulating fetuin-A is positively associated with dyslipidemia as well as fatty liver in humans and rodents.^(25,28) In addition, obesity correlated with high fetuin-A concentration.⁽²⁹⁾ However, CO feeding reduced plasma fetuin-A level associated with hepatic expression in KK mice, although the body weight, plasma lipid level, and liver fat content did not improve in these mice. The hepatic expression of fatty acid synthase and stearoyl-CoA desaturase 1 increased in CO-fed KK mice. These are the rate-limiting enzymes that catalyze the biosynthesis of fatty acids used as the main substrates for the synthesis of hepatic TG.^(30,31) Consistently, the CO diet increased hepatic FFA level and TG content ($p = 0.0611$) compared with the LSO diet in KK mice. Several studies have used a high-fat diet (24–35% from lipids in total diet) with or without CO and represented the beneficial effects of its CO oil on obesity, dyslipidemia, and fatty liver in BL6 mice.^(6,32,33) By contrast, CO feeding decreased plasma TG level but increased blood glucose level and plasma TC level in *db/db* mice, a severe type 2 diabetic model animal, that were fed a standard chow diet

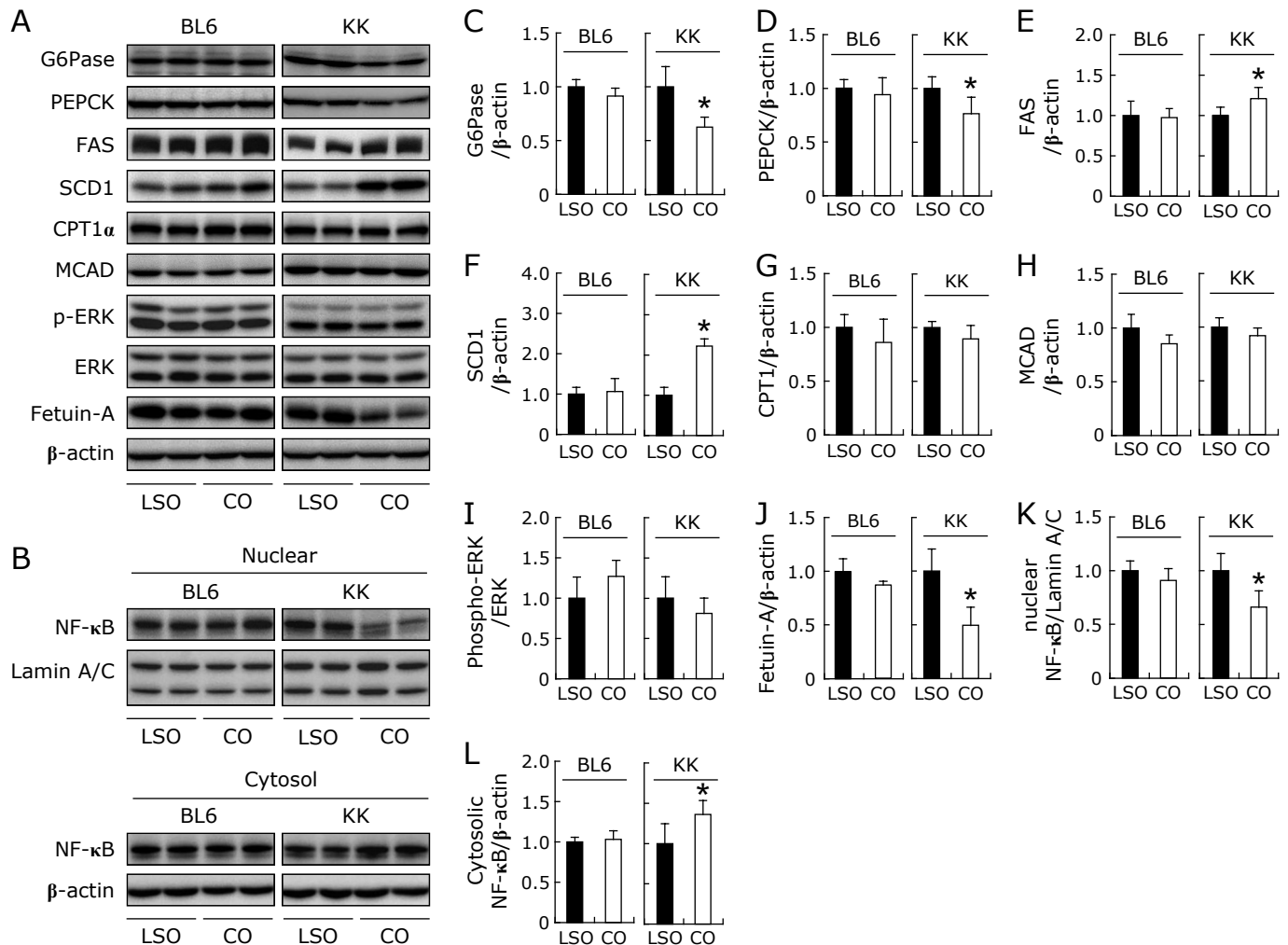


Fig. 2. Hepatic expression of proteins in C57BL/6J and KK mice. Representative blots of immunoblot analysis in the total fraction (A) and nuclear-cytosolic fraction (B). Expression of G6Pase (C), PEPCCK (D), FAS (E), SCD1 (F), CPT1 (G), MCAD (H), ratio of phospho-ERK 1/2 and total ERK 1/2 (I), fetuin-A (J), nuclear NF- κ B (K), and cytosolic NF- κ B (L). Data are presented as the mean \pm SD ($n = 5$) and fold-change of the mean value of the LSO group. * $p < 0.05$ vs LSO group. Comparisons of two data in each strain were performed using the unpaired Student's t test. BL6, C57BL/6J mouse; CO, coconut oil; CPT1, carnitine palmitoyl transferase 1; ERK, extracellular signal-regulated kinases; FAS, fatty acid synthase; G6Pase, glucose-6-phosphatase; LSO, lard/safflower oil; MCAD, medium-chain acyl-CoA dehydrogenase; NF- κ B, nuclear factor-kappa B; PEPCCK, phosphoenolpyruvate carboxykinase; SCD1, stearoyl-CoA desaturase 1.

(10.7% from lipids in total diet) with CO.⁽³⁴⁾ The KK mouse is also an animal model of mild obesity and type 2 diabetes. In our study, CO feeding did not improve lipid levels in the plasma and liver in KK mice. On the basis of these findings, it is reasonable to assume that CO consumption showed positive and negative effects on lipid metabolism depending on the health condition of the mouse strain and the total amount of daily lipid intake. Taken together, the reduction of fetuin-A in the plasma and liver by CO feeding was not mediated through at least in part improvement of obesity, dyslipidemia, and fatty liver in CO-fed KK mice.

The NF- κ B-dependent pathway is an important mediator of fatty acid-induced fetuin-A transcription in hepatocyte.⁽¹²⁾ TLR4 signaling pathway is one of the triggers for the translocation of NF- κ B to the nucleus.⁽³⁵⁾ It has been reported that not only palmitic acid but also lauric acid, rich in CO, activated TLR4 with the interplay of fetuin-A.⁽³⁶⁾ Although KK mice were fed a high amount of lauric acid from the CO diet, they showed a decrease in the expression of fetuin-A, associated with suppressing NF- κ B translocation to the nucleus in the liver, but not in the eWAT. These findings suggest that CO intake reduced

hepatic fetuin-A production independent of the TLR4/NF- κ B signaling pathway. Fetuin-A expression in HepG2, a human liver cell line, was induced by high levels of glucose through the ERK1/2 signaling pathway.⁽¹³⁾ Compared with the LSO diet, the CO diet decreased blood glucose level in KK mice, assuming that these mice showed attenuation of ERK1/2 activation in the liver. Unexpectedly, no significant change was observed in the phosphorylation of hepatic ERK1/2 between the LSO and CO groups in KK mice. Our findings highlight that CO feeding downregulated fetuin-A expression in the liver, but not in the eWAT, and inhibited the nuclear translocation of NF- κ B in KK mice. Dietary MCFAs are absorbed from the gut and transported directly to the liver through the portal vein, making them more readily available to the liver than other tissues, such as the heart and skeletal muscle.⁽³⁷⁾ Therefore, the liver may be more susceptible to dietary CO, rich in MCFAs, than eWAT in mice. Further investigations are needed to clarify the mechanism underlying the influence of CO consumption on fetuin-A production.

In conclusion, our data demonstrated that CO feeding downregulated the hepatic expression of fetuin-A and reduced the

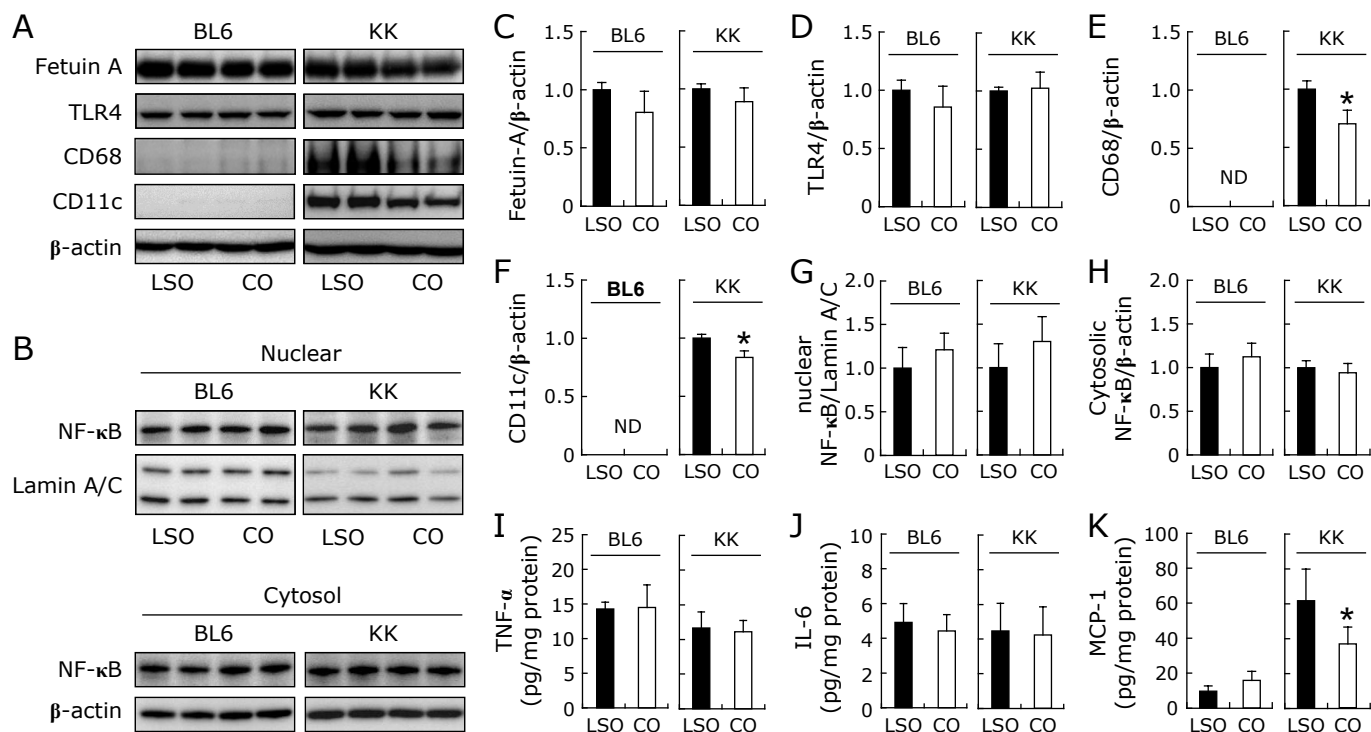


Fig. 3. eWAT expression in C57BL/6J and KK mice. Representative blots of immunoblot analysis of total fraction (A) and nuclear-cytosolic fraction (B). Expression of fetuin-A (C), TLR4 (D), CD68 (E), CD11c (F), nuclear NF-κB (G), and cytosolic NF-κB (H). Levels of TNF-α (I), IL-6 (J), and MCP-1 (K) in tissue homogenates. Data are presented as the mean ± SD ($n = 5$) and fold-change of the mean value of the LSO group. * $p < 0.05$ vs LSO group. Comparisons of two data in each strain were performed using the unpaired Student's t test. BL6, C57BL/6J mouse; CO, coconut oil; IL-6, interleukin-6; LSO, lard/safflower oil; MCP-1, monocyte chemoattractant protein-1; ND, not detected; NF-κB, nuclear factor-kappa B; TNF-α, tumor-necrosis factor-alpha; TLR4, toll-like receptor 4.

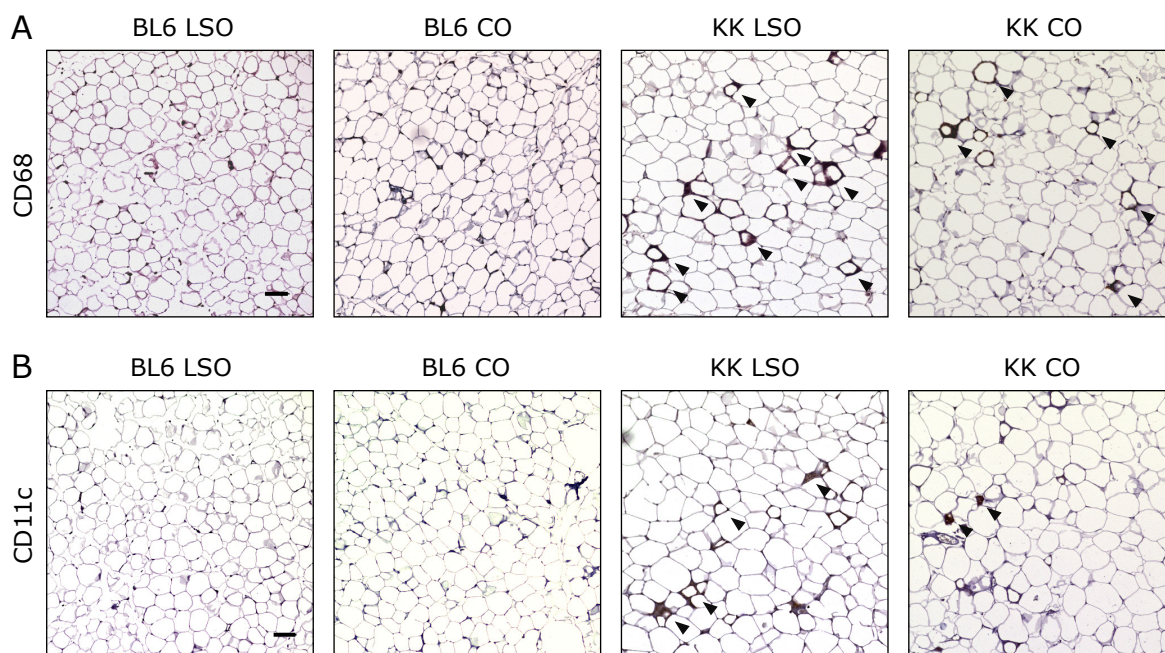


Fig. 4. Representative images of immunostaining in the eWAT of C57BL/6J and KK mice. Stained sections of CD68 (A) and CD11c (B). Arrow heads indicate immunostained positive cells for CD68 or CD11c. Scale bar: 100 μm. Original magnification: 100x. BL6, C57BL/6J mouse; CO, coconut oil; LSO, lard/safflower oil.

plasma levels of fetuin-A in KK mice. M1 macrophage infiltration in eWAT was inhibited in CO-fed KK mice associated with a decrease in MCP-1 levels. However, CO consumption did not improve insulin resistance. Further studies, including factors such as severity of obesity and diabetes, strain of mouse, and amount of CO intake, are needed to evaluate the benefits of CO consumption on glucose and lipid metabolism.

Author Contributions

YI: analysis, conceptualization, data curation, writing – original draft; CK: analysis, data curation; TT: analysis, data curation; HU: analysis, data curation, writing – review & editing; SH: analysis, data curation, writing – review & editing; TO: writing – review & editing; HK: writing – review & editing; NY: writing – review & editing, supervision, project administration.

References

- Orsavova J, Misurcova L, Ambrozova JV, Vicha R, Mlcek J. Fatty acids composition of vegetable oils and its contribution to dietary energy intake and dependence of cardiovascular mortality on dietary intake of fatty acids. *Int J Mol Sci* 2015; **16**: 12871–12890.
- DeLany JP, Windhauser MM, Champagne CM, Bray GA. Differential oxidation of individual dietary fatty acids in humans. *Am J Clin Nutr* 2000; **72**: 905–911.
- Deen A, Visvanathan R, Wickramarachchi D, et al. Chemical composition and health benefits of coconut oil: an overview. *J Sci Food Agric* 2021; **101**: 2182–2193.
- Zicker MC, Silveira ALM, Lacerda DR, et al. Virgin coconut oil is effective to treat metabolic and inflammatory dysfunction induced by high refined carbohydrate-containing diet in mice. *J Nutr Biochem* 2019; **63**: 117–128.
- Ngala RA, Ampom I, Sakyi SA, Anto EO. Effect of dietary vegetable oil consumption on blood glucose levels, lipid profile and weight in diabetic mice: an experimental case—control study. *BMC Nutr* 2016; **2**: 28.
- Lee EJ, Oh H, Kang BG, et al. Lipid-lowering effects of medium-chain triglyceride-enriched coconut oil in combination with licorice extracts in experimental hyperlipidemic mice. *J Agric Food Chem* 2018; **66**: 10447–10457.
- Pan D, Li G, Jiang C, Hu J, Hu X. Regulatory mechanisms of macrophage polarization in adipose tissue. *Front Immunol* 2023; **14**: 1149366.
- Ströher DJ, de Oliveira MF, Martinez-Oliveira P, et al. Virgin coconut oil associated with high-fat diet induces metabolic dysfunctions, adipose inflammation, and hepatic lipid accumulation. *J Med Food* 2020; **23**: 689–698.
- Rodríguez-García C, Sánchez-Quesada C, Algarra I, Gaforio JJ. Differential Immunometabolic effects of high-fat diets containing coconut, sunflower, and extra virgin olive oils in female mice. *Mol Nutr Food Res* 2022; **66**: e2200082.
- Dhanasekara CS, Nelson A, Spradley M, et al. Effects of consumption of coconut oil or coconut on glycemic control and insulin sensitivity: a systematic review and meta-analysis of interventional trials. *Nutr Metab Cardiovasc Dis* 2022; **32**: 53–68.
- Chekol Abebe E, Tilahun Muche Z, Behaile T/Mariam A, et al. The structure, biosynthesis, and biological roles of fetuin-A: a review. *Front Cell Dev Biol* 2022; **10**: 945287.
- Dasgupta S, Bhattacharya S, Biswas A, et al. NF-kappaB mediates lipid-induced fetuin-A expression in hepatocytes that impairs adipocyte function effecting insulin resistance. *Biochem J* 2010; **429**: 451–462.
- Takata H, Ikeda Y, Suehiro T, et al. High glucose induces transactivation of the $\alpha 2$ -HS glycoprotein gene through the ERK1/2 signaling pathway. *J Atheroscler Thromb* 2009; **16**: 448–456.
- Heinrichsdorff J, Olefsky JM. Fetuin-A: the missing link in lipid-induced inflammation. *Nat Med* 2012; **18**: 1182–1183.
- Sardana O, Goyal R, Bedi O. Molecular and pathobiological involvement of fetuin-A in the pathogenesis of NAFLD. *Inflammopharmacology* 2021; **29**: 1061–1074.
- Öner-Iyidoğan Y, Koçak H, Seyidhanoglu M, et al. Curcumin prevents liver fat accumulation and serum fetuin-A increase in rats fed a high-fat diet. *J*

Acknowledgments

We would like to thank Ms. Kodama, Mr. Takei, and Mr. Yoshikawa for their technical support and animal care. We also acknowledge Nobuhiro Wada for his technical advice of nuclear extraction. We are grateful to Enago (www.enago.com) for the English language review. This study was in part supported by the Institute of Laboratory Animals of Tokyo Women's Medical University. In this research work we used Institute for Comprehensive Medical Sciences (ICMS), Tokyo Women's Medical University.

Conflict of Interest

No potential conflicts of interest were disclosed.

- Physiol Biochem* 2013; **69**: 677–686.
- Lee HJ, Lim Y, Yang SJ. Involvement of resveratrol in crosstalk between adipokine adiponectin and hepatokine fetuin-A *in vivo* and *in vitro*. *J Nutr Biochem* 2015; **26**: 1254–1260.
- Iizuka Y, Hirako S, Kim H, Wada N, Ohsaki Y, Yanagisawa N. Fish oil-derived n-3 polyunsaturated fatty acids downregulate aquaporin 9 protein expression of liver and white adipose tissues in diabetic KK mice and 3T3-L1 adipocytes. *J Nutr Biochem* 2024; **124**: 109514.
- Folch J, Lees M, Sloane Stanley GH. A simple method for the isolation and purification of total lipides from animal tissues. *J Biol Chem* 1957; **226**: 497–509.
- Wada N, Hirako S, Takenoya F, Kageyama H, Okabe M, Shioda S. Leptin and its receptors. *J Chem Neuroanat* 2014; **61–62**: 191–199.
- Park S, Shin S, Lim Y, Shin JH, Seong JK, Han SN. Korean pine nut oil attenuated hepatic triacylglycerol accumulation in high-fat diet-induced obese mice. *Nutrients* 2016; **8**: 59.
- Santos-González M, López-Miranda J, Pérez-Jiménez F, Navas P, Villalba JM. Dietary oil modifies the plasma proteome during aging in the rat. *Age (Dordr)* 2012; **34**: 341–358.
- Dittrich M, Jahreis G, Bothor K, et al. Benefits of foods supplemented with vegetable oils rich in α -linolenic, stearidonic or docosahexaenoic acid in hypertriglyceridemic subjects: a double-blind, randomized, controlled trial. *Eur J Nutr* 2015; **54**: 881–893.
- Zhang X, Yang S, Chen J, Su Z. Unraveling the regulation of hepatic gluconeogenesis. *Front Endocrinol (Lausanne)* 2019; **9**: 802.
- Hirako S, Wakayama Y, Kim H, et al. Association of aquaporin 7 and 9 with obesity and fatty liver in *db/db* mice. *Zoolog Sci* 2023; **40**: 455–462.
- Hasegawa Y. New perspectives on obesity-induced adipose tissue fibrosis and related clinical manifestations. *Endocr J* 2022; **69**: 739–748.
- Chatterjee P, Seal S, Mukherjee S, et al. Adipocyte fetuin-A contributes to macrophage migration into adipose tissue and polarization of macrophages. *J Biol Chem* 2013; **288**: 28324–28330.
- Peng K, Mo Z, Tian G. Serum lipid abnormalities and nonalcoholic fatty liver disease in adult males. *Am J Med Sci* 2017; **353**: 236–241.
- Brix JM, Stingl H, Höllerl F, Scherthaner GH, Kopp HP, Scherthaner G. Elevated fetuin-A concentrations in morbid obesity decrease after dramatic weight loss. *J Clin Endocrinol Metab* 2010; **95**: 4877–4881.
- Innocenzi D, Alò PL, Balzani A, et al. Fatty acid synthase expression in melanoma. *J Cutan Pathol* 2003; **30**: 23–28.
- Dobrzyn A, Ntambi JM. Stearoyl-CoA desaturase as a new drug target for obesity treatment. *Obes Rev* 2005; **6**: 169–174.
- Wang ME, Singh BK, Hsu MC, et al. Increasing dietary medium-chain fatty acid ratio mitigates high-fat diet-induced non-alcoholic steatohepatitis by regulating autophagy. *Sci Rep* 2017; **7**: 13999.
- Gao Y, Liu Y, Han X, et al. Coconut oil and medium-chain fatty acids attenuate high-fat diet-induced obesity in mice through increased thermogenesis by activating brown adipose tissue. *Front Nutr* 2022; **9**: 896021.
- Martínez-Carrillo BE, Mondragón-Velásquez T, Ramírez-Durán N, et al. Changes in metabolic regulation and the microbiota composition after supple-

- mentation with different fatty acids in db/db mice. *Int J Food Sci* 2022; **2022**: 3336941.
- 35 Rogero MM, Calder PC. Obesity, inflammation, toll-like receptor 4 and fatty acids. *Nutrients* 2018; **10**: 432.
- 36 Huang S, Rutkowsky JM, Snodgrass RG, *et al*. Saturated fatty acids activate TLR-mediated proinflammatory signaling pathways. *J Lipid Res* 2012; **53**: 2002–2013.
- 37 Pereyra AS, McLaughlin KL, Buddo KA, Ellis JM. Medium-chain fatty acid

oxidation is independent of L-carnitine in liver and kidney but not in heart and skeletal muscle. *Am J Physiol Gastrointest Liver Physiol* 2023; **325**: G287–G294.



This is an open access article distributed under the terms of the Creative Commons Attribution-NonCommercial-NoDerivatives License (<http://creativecommons.org/licenses/by-nc-nd/4.0/>).
